Pharmaceutical Research, Vol. 24, No. 3, March 2007 (© 2007)
DOI: 10.1007/s11095-006-9171-6

Research Paper

Paclitaxel-2′-Ethylcarbonate Prodrug Can Circumvent P-glycoprotein-mediated Cellular Efflux to Increase Drug Cytotoxicity

Tadatoshi Tanino,[1] Akihiro Nawa,[2] Eisaku Kondo,[3] Fumitaka Kikkawa,[2] Tohru Daikoku,[4] Tatsuya Tsurumi,[4] ChenHong Luo,[2] Yukihiro Nishiyama,[2] Yuki Takayanagi,[5] Katuhiko Nishimori,[5] Seiji Ichida,[1] Tetsuyuki Wada,[1] Yasuyoshi Miki,[1] and Masahiro Iwaki[1,6]

Received June 15, 2006; accepted September 26, 2006; published online January 24, 2007

Purpose. The aim of the study was to investigate whether 2′-ethylcarbonate-linked paclitaxel (TAX-2′-Et) circumvents P-glycoprotein (P-gp)-mediated cellular efflux and cytotoxicity enhanced by TAX-2′-Et activation within human culture cells transfected with a rabbit liver carboxylesterase (Ra-CES) cDNA.
Materials and Methods. TAX-2′-Et transport was characterized in a human colon carcinoma cell line (Caco-2) and paclitaxel (TAX)-resistant ovarian carcinoma cells (SKOV3/TAX60). Expression of P-gp, multidrug resistance protein (MRP) 2 and Ra-CES was detected by Western blotting. Cytotoxicity against Ra-CES-expressing cells and cellular amount of TAX produced were determined by MTT assay and using HPLC, respectively.
Results. Unlike rhodamine123 and TAX, TAX-2′-Et did not exhibit polarized transport in the Caco-2 cells in the absence or presence of verapamil. P-gp levels were expressed much higher in the SKOV3/TAX60 cells than in the Caco-2 cells. MRP2 protein was not detectable in the SKOV3/TAX60 cells. Uptake by the SKOV3/TAX60 cells was similar in quantity to the amount internalized by P-gp-negative SKOV3 cells. In the SKOV3/TAX60 cells, cellular uptake of TAX-2′-Et was not altered regardless of the absence or presence of verapamil. The cytotoxicity to the untransfected SKOV3 cells induced by TAX-2′-Et was significantly lower than that induced by TAX. In the Ra-CES-expressing SKOV3 line, the EC_{50} value of TAX (10.6 nM) was approximately four-fold higher than that of TAX-2′-Et (2.5 nM). Transfection of Ra-CES into another TAX-resistant ovarian carcinoma cells (KOC-7c) conferred a high level of TAX-2′-Et cytotoxicity via prodrug activation. The intracellular levels of TAX produced from TAX-2′-Et in the Ra-CES-positive KOC-7c cells significantly increased compared with the levels seen in exposure of the untransfected KOC-7c cells to TAX.
Conclusions. TAX-2′-Et can circumvent P-gp-associated cellular efflux of TAX. TAX-2′-Et is converted into TAX by the Ra-CES, supporting its potential use as a theoretical GDEPT strategy for cancer cells expressing high levels of P-gp. The TAX-2′-Et prodrug efficiently increased the amount of intracellular TAX, which mediates tumor cell death.

KEY WORDS: carboxylesterase-prodrug; gene-directed enzyme prodrug therapy; growth inhibition; paclitaxel; P-glycoprotein.

[1] School of Pharmaceutical Sciences, Kinki University, 3-4-1 Kowakae, Higashi-Osaka, Osaka 577-8502, Japan.
[2] Nagoya University Graduate School of Medicine, 65 Tsurumai-cho, Shouwa-ku, Nagoya 466-8550, Japan.
[3] Okayama University Medical School, Okayama 700-8558, Japan.
[4] Aichi Cancer Center Research Institute, Chikusa-ku, Nagoya 464-8681, Japan.
[5] Graduate School of Agricultural Science, Tohoku University, 1-1 Tsutsumidori-Amamiyamachi, Sendai 981-8555, Japan.
[6] To whom correspondence should be addressed. (e-mail: iwaki@phar.kindai.ac.jp)

ABBREVIATIONS: BCRP, Breast cancer resistance protein; Caco-2, Human colon carcinoma cells; CPT-11, Irinotecan; DMSO, Dimethylsulfoxide; EC_{50}, Half of the maximal cell death; GDEPT, Gene-directed enzyme prodrug therapy; HepG2, Human hepatoma cells; HPLC, High-performance liquid chromatography; KOC-7c, Human clear cell carcinoma of ovary cell line; MRP, Multidrug resistance protein; MTT, 3-(4,5-dimethylthiazol-2-yl)-2,5-diphenyltetrazolium bromide; P_{app}, Apparent permeability coefficient; P-gp, P-glycoprotein; Ra-CES, A carboxylesterase isolated from rabbit liver; Rh123, Rhodamine 123; SKOV3, Human ovarian carcinoma cells; SKOV3/TAX60, Paclitaxel-resistant ovarian carcinoma cells; TAX, Paclitaxel; TAX-2′-Et, 2′-ethylcarbonate-linked paclitaxel; TEER, Trans-epithelial electrical resistance.

INTRODUCTION

Paclitaxel (Taxol^R, TAX) has been successfully used for the treatment of a variety of tumors, including those of the breast, ovary and lung (1). For patients with epithelial ovarian cancer, combination therapy with TAX and platinum agents is the recommended first-line chemotherapy regiment (2,3). The mechanisms of resistance to TAX and other microtuble-stabilizing agents that have been characterized previously in human cell lines include expression of P-glycoprotein (P-gp), mutations in the cellular target of TAX (4), class III β-tublin expression level (5) and increased microtubule dynamics (6). The role of these various forms of TAX resistance, particularly their

contribution to resistance in the cancer patient, is not clear. However, overexpression of P-gp facilitates the export of TAX by multidrug-resistant cells, reducing the intracellular drug concentration and permitting the survival of tumor cells at drug concentrations that are usually toxic (7–10). To reverse the P-gp-mediated drug resistance, strategies of utilizing potent P-gp inhibitors (verapamil and cyclosporin A) or a modulator (PSC 833) have been examined in mice and human (11–14). Unfortunately, the inhibitors and PSC 833 significantly alter the pharmacokinetics of TAX.

Several gene-directed enzyme prodrug therapy (GDEPT) strategies have been developed combining cytosine deaminase and 5-fluorocytosine, cytochrome P450 2B1 and cyclophosphamide, and carboxylesterase (CES) and irinotecan (CPT-11) (15). Although the activated forms of these prodrugs are not a frontline therapy for the treatment of ovarian cancer, it would be beneficial to develop a more effective prodrug-enzyme combination for the treatment of this disease. Many prodrugs and derivatives of TAX have been developed based on the chemical modification of the hydroxyl groups at position 7 of the baccatin core and position 2′ of the TAX side chain (16,17). Ueda *et al.* (17) demonstrated that TAX-2′-carbonates were 2–10 times less cytotoxic than TAX against a human colon cancer cell line. Of these prodrugs, 2′-ethylcarbonate-conjugated TAX (TAX-2′-Et, Fig. 1) exhibited the most rapid accumulation into the cells. Chemical modifications in the baccatin portion of TAX also decrease affinity for P-gp transporter system (18). Our enzymatic stability studies preliminarily showed that TAX-2′-Et was stable in both human and rabbit sera. A CES isolated from rabbit liver (Ra-CES) efficiently converted TAX-2′-Et to the parental drug. Our attention is focused on combination of TAX-2′-Et and Ra-CES for development of a new GDEPT. If TAX-2′-Et as well as TAX is greatly exported through the efflux pump of P-gp, our GDEPT strategy for treatment of ovarian cancer may fail to improve therapeutic efficacy that depends on increased levels of intracellular TAX. Therefore, it is most important in our strategy to utilize prodrugs that can circumvent P-gp-mediated efflux of TAX.

In a present study, we investigated the transport of TAX-2′-Et in a human colon carcinoma cell line (Caco-2) that expresses P-gp. We also analyzed the uptake of TAX-2′-Et into both human ovarian carcinoma cells (SKOV3) and its TAX-resistant cells (SKOV3/TAX60). TAX-2′-Et activation, mediated by the conversion of TAX-2′-Et to TAX, was measured as *in vitro* cytotoxicity to both TAX-sensitive SKOV3 cells and a human clear cell carcinoma of the ovary cell line (TAX-resistant cells, KOC-7c), which were transfected with a plasmid encoding Ra-CES.

MATERIALS AND METHODS

TAX-2′-Et Synthesis

TAX-2′-Et was prepared by the method reported by Ueda *et al.* (17). The structural assignment of TAX-2′-Et was made on the basis of its ^{1}H NMR spectrum and mass spectrum.

Cell Culture

Caco-2 cells, purchased from the American Type Culture Collection (ATCC, Rockville, MD), were used at passage 18–28. Cells were grown in culture medium consisting of Dulbecco's modified Eagle's medium (DMEM, Nacalai Tesque Co., Kyoto, Japan) supplemented with 0.1 mM non-essential amino acids, 10% heat-inactivated fetal bovine serum (FBS), 100 U/ml penicillin G and 0.1 mg/ml streptomycin sulfate.

SKOV3 cells were obtained from the Memorial Sloan–Kettering Cancer Center (New York, NY). SKOV3 cells transfected with the CES gene under the control of the Tet-off system (BD Biosciences Clontech, CA, USA) were maintained in DMEM containing 10% FBS, 0.5 mg/ml G418, 2 μg/ml doxycycline (Dox), 0.5 mg/ml hygromycin (hyg), 100

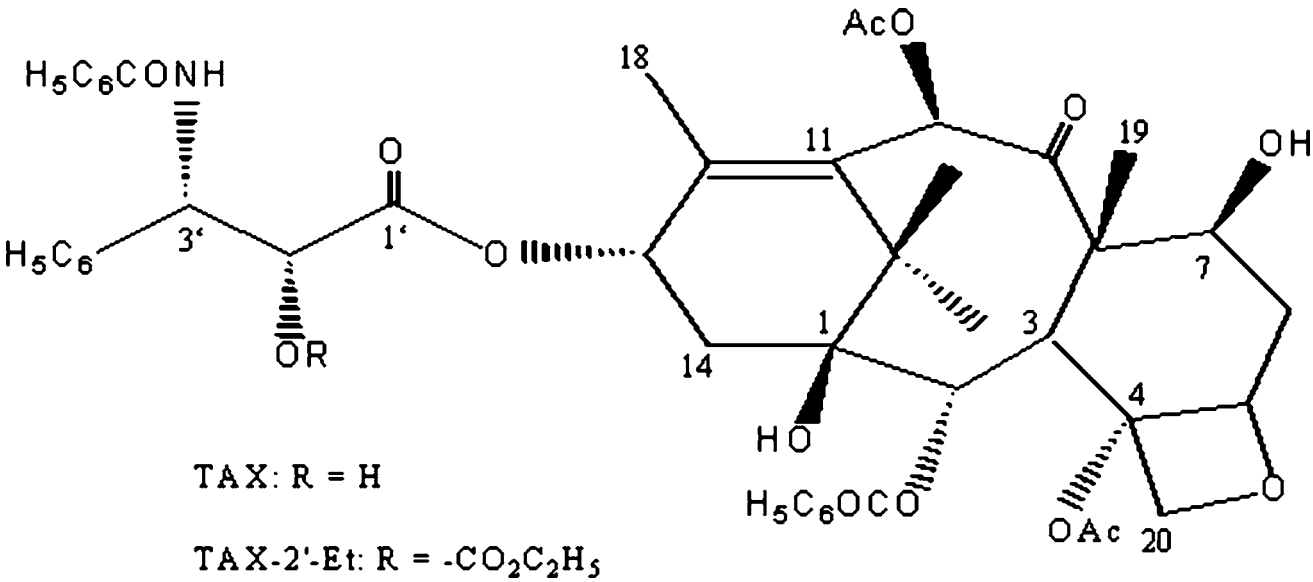

Fig. 1. Chemical structures of TAX and TAX-2′-Et.

U/ml penicillin G, and 0.1 mg/ml streptomycin sulfate (Tet-on medium). The expression of functional CES was then initiated by replacement of culture medium with Tet-off medium, which lacked Dox. The parental SKOV3 cells were grown in DMEM containing 10% FBS, 100 U/ml penicillin G and 0.1 mg/ml streptomycin sulfate. SKOV3/TAX60 cells were selected from the SKOV3 cell population following stepwise increases in TAX concentrations from 0.1 to 60 nM.

KOC-7c cells (a gift from Dr. Kigawa, Tottori University) were maintained as described by Itamochi *et al.* (19).

Human hepatoma cell line HepG2 purchased from the American Type Culture Collection (ATCC, Rockville, MD), were used at passage 52–56. The cells were grown in culture medium consisting of RPMI-1640 (Sigma Chemical Co., St. Louis, MO, USA) supplemented with 10% heat-inactivated FBS, 100 U/ml penicillin G and 0.1 mg/ml streptomycin sulfate.

Cloning of a Ra-CES cDNA and Construction of Its Expression Vector

A cDNA encoding a Ra-CES was isolated according to the method reported by Potter *et al.* (20). A cDNA library was prepared from total rabbit liver poly $(A)^+$ RNA (BD Biosciences Clontech, CA, USA) with a cDNA synthesis kit (TaKaRa Bio Inc., Shiga, Japan) using random primers. The full-length Ra-CES cDNA was amplified from the library using specific oligonucleotide primers and TaKaRa LA taq™ polymerase (TaKaRa Bio. Inc., Shiga, Japan) under the conditions described (20). The ~1,700 bp product was ligated into the pCR2.1 vector (Invitrogen Co., CA, USA). The Ra-CES cDNA sequence was confirmed using a DNA sequencing kit (Applied Biosystems, CA, USA) and a 3100 Genetic Analyzer (Applied Biosystem, CA, USA). The cDNA was inserted in frame into pCMVTag2 expression vector (STRATAGENE, USA) at EcoR1 site, then, a fragment containing Ra-CES was ligated into pTRE2 hyg expression vector (BD Biosciences Clontech, CA, USA) at Not1-Cla1 site. We named this vector pTRE2 hyg-Ra-CES.

Stable Transfection of Ra-CES in Tet-off System

SKOV3 cells that harbor a homozygous deletion of the p53 gene were obtained from the ATCC. SKOV3 cells were transfected with the pTet-off plasmid (BD Biosciences Clontech, CA, USA) using LipofectAMINE™ Plus™ Reagent (Invitrogen Co., CA, USA) according to the manufacture's protocol. From the isolated G418-resistant clones, we screened for those with low background expression and high Dox dependent induction of expression following transient transfection with the pTRE2-Luc plasmid (BD Biosciences Clontech, CA, USA). SKOV3 cells containing the pTet-off plasmid were also transfected with the pTRE2 hyg-Ra-CES expression vector using LipofectAMINE™. Transfected clones resistant to 500 μg/ml hyg B treatment were tested for CES activity in the presence or absence of 1 μg/ml Dox. Clones expressing the lowest basal levels of CES activity in the presence of Dox and the highest levels of CES activity induced by the absence of Dox were maintained continuously in the presence of Dox until experimentation.

Transient Transfection of pHGCX-Ra-CES into KOC-7c Cells

pHGCX, a eukaryotic expression vector encoding enhanced green fluorescence protein under the control of the HSV-1 IE4/5 promoter, was kindly provided by Dr. Saeki (Harvard Medical School). The Ra-CES fragment containing Kozak and FLAG sequences derived from pTRE2 hyg-Ra-CES was ligated into Nhe1-EcoR1 site of pHGCX that express FLAG-Ra-CES fusion protein under the control of the CMV IE promoter, to generate pHGCX-Ra-CES (Fig. 5a and b). KOC-7c cells (5×10^6) were transfected with 2 μg empty pHGCX or pHGCX-Ra-CES using Lipofect AMINE™ Plus reagent (Invitrogen Co., California, USA).

Carboxylesterase Assay

We measured carboxylesterase activity as described by Hennebelle *et al.* (21). The enzymatic reaction was initiated by the addition of *p*-nitrophenylacetate as a substrate. Optical density at 405 nm was measured continuously for 10 min at 37°C using a microplate reader (Wellreader SK601, Seikagaku Co., Tokyo, Japan). Enzymatic activities were normalized to the levels of total cellular protein.

Transport Studies

Caco-2 cells were plated at a density of 6.4×10^4 cells/cm^2 on polycarbonate filters. Monolayers were utilized for transport experiments 21–25 days after seeding. TAX and TAX-2′-Et were dissolved in dimethylsulfoxide (DMSO) to yield a final concentration of 0.5% DMSO, then diluted in Hanks' balanced salt solution (HBSS) (pH 7.4) containing 25 mM 2-[4-(2-hydroxyethyl)-1-piperazinyl] ethanesulfonic acid to a final concentration of 3.5 μM. At the indicated times, the incubation medium was removed from the contralateral side. Simultaneously, we monitored the polarized transport of a P-gp substrate, rhodamine123 (Rh123, 5 mM), under the same conditions as a positive control. To examine transport inhibition, 200 μM verapamil was added to both sides of the monolayer in separate experiments. The integrity of the monolayers was monitored by the transepithelial electrical resistance (TEER) using Millicell-ERS (Millipore, Bedford, MA, USA). The TEER values of monolayers used were >400 Ω cm^2. For assay measuring TAX and the prodrug concentrations, TAX and TAX-2′-Et in the collected incubation solutions were extracted with diethyl ether. After the organic phase was evaporated, the residue was redissolved in the mobile phase for examination by high-performance liquid chromatography (HPLC) assay.

Cellular Uptake

SKOV3 and SKOV3/TAX60 cell lines were seeded onto dishes at a density of 5×10^4 cells/cm^2 and then were maintained for 24 h. HepG2 cells, seeded at a density of 2.5×10^4 cells/cm^2), were usually used after 5–7 days of culture, when confluency and maximal polarity had been reached. Uptake experiments were initiated by the addition of fresh HBSS containing 3.5 μM TAX or TAX-2′-Et.

Verapamil (final concentration, 200 μM) and probenecid (final concentration, 250 μM) were also added to the SKOV3/TAX60 and HepG2 cells, respectively. After 1-h incubation, cells were immediately washed twice with ice-cold phosphate-buffered saline (PBS). Cells were deproteinized with methanol and harvested with a cell scraper. All cell suspensions were disrupted by sonication for 20 s; the resulting solutions were centrifuged at 19,000 rpm for 20 min. An aliquot (1.3 ml) of each supernatant was evaporated under reduced pressure. The residue was reconstituted in 35 mM ammonium acetate buffer (pH 5.0) containing medazepam, an internal standard. TAX and TAX-2′-Et were extracted in diethyl ether. After removal of the organic phase, the residue was dissolved in the mobile phase used for the HPLC assay. The reconstituted solutions were injected onto a HPLC column for analysis.

Western Blotting

For Western blot analysis of P-gp and multidrug resistance protein (MRP) 2, the five cells grown in 100-mm dishes were lysed in 300 μl of a buffer containing 1% Triton X-100 and 20 mM Tris–HCl (pH 7.6) supplemented with a cocktail of protease inhibitors (Sigma, USA), 1 mM phenylmethylsulfonyl fluoride and 1 M ethylenediamine-*N*,*N*,*N*′,*N*′-tetraacetic acid salts. Equal amounts (50 μg) of proteins in cell lysates were electrophoresed on gels of SuperSept™ 5–20% (Wako Pure Chemicals Co., Ltd., Osaka, Japan).

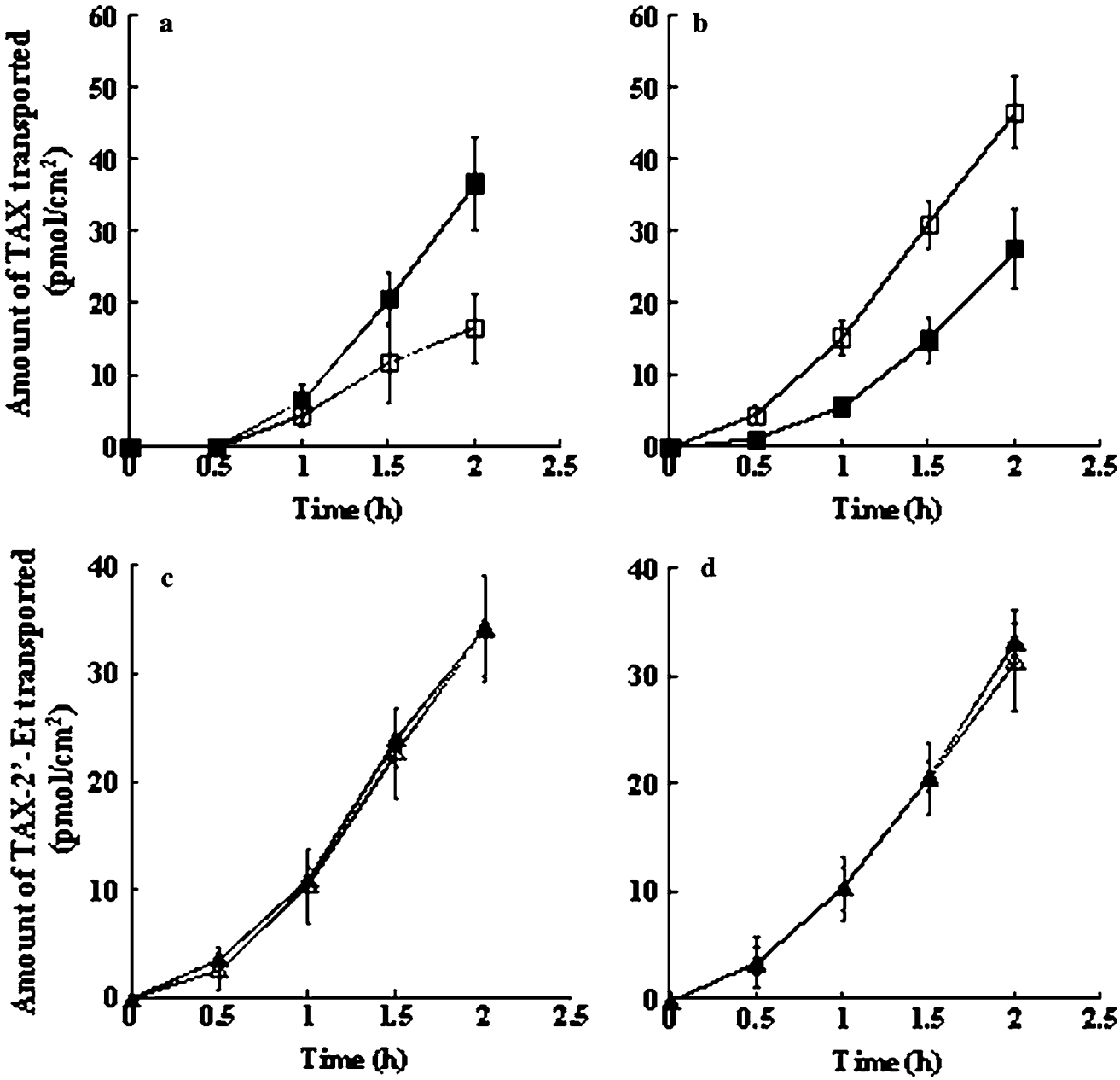

Fig. 2. Transepithelial flux of TAX (a, b) and TAX-2′-Et (c, d) across Caco-2 cell monolayers in a transwell system. Cells were incubated in the absence (*open square*, *open triangle*) and presence (*filled square*, *filled triangle*) of verapamil. **a** and **c** Apical-to-basolateral flux. **b** and **d** Basolateral-to-apical flux. The results are given with standard deviation (n=3–4).

Proteins were transferred onto polyvinylidene difluoride membranes. Blots were probed for 1 h with a 1:25 dilution of a monoclonal mouse anti-P-gp antibody, clone C219 (Signet Pathology Systems, Inc., Dedham, Massachusetts, USA) or 1:50 dilution of monoclonal mouse antibody to human MRP2 (M_2III-6, Alexis Biochemicals, Nottingham, UK). Membranes were washed in TBST [25 mM Tris–HCl (pH 7.5), 150 mM NaCl and 0.1% Tween 20], containing 1% non-fat dry milk and incubated with a 1:2,000 dilution of horseradish peroxidase-conjugated anti-mouse secondary antibody (Amersham Biosciences, Buckingham, UK) for 1 h. After three washes with TBST, bound antibody was detected by enhanced chemiluminescence (ECL plus, Amersham Biosciences, Buckingham, UK) and visualized on X-ray film.

Western blot analysis for Ra-CES was also performed according to the procedure described above. Total cell extracts were prepared from KOC-7c cells or pHGCX-Ra-CES transfected KOC-7c cells. Fifty micrograms of proteins for each samples were electrophoresed, and electroblotted onto polyvinylidene difluoride membranes. The membranes were hybridized with a 1:1,000 dilution of a monoclonal mouse ANTI-FLAG M2 antibody (Sigma, USA). After the addition of anti-mouse IgG (BIOSOURCE, CA, USA), the membranes were detected with the ECL system.

Growth Inhibitory Effects

Untransfected (1×10^4 cells/well) or transfected (2×10^4 cells/well) SKOV3 cells were plated in 96 well plates and incubated for 24 h. After two washes with PBS, untransfected SKOV3 cells were incubated in solutions containing TAX or TAX-2′-Et at concentrations ranging from 0.5 to 3,500 nM. Transfected cells were incubated in Tet-off medium for 48 h to induce the expression of functional CES before treatment with the drug solutions. After 72 h, 3-(4,5-dimethylthiazol-2-yl)-2,5-diphenyltetrazolium bromide (MTT) (2 mg/ml) solution was added to each well for an additional 3 h. After removal of the medium, DMSO was added to each well to dissolve the formazan crystals. We measured the optical density at 570 nm using the microplate reader.

The sensitivity of the transient transfected and untransfected KOC-7c cells to TAX or TAX-2′-Et was evaluated using the CellTiter 96^R AQueous One Solution Cell Proliferation Assay kit (Promega Co., WI, USA). Twenty-

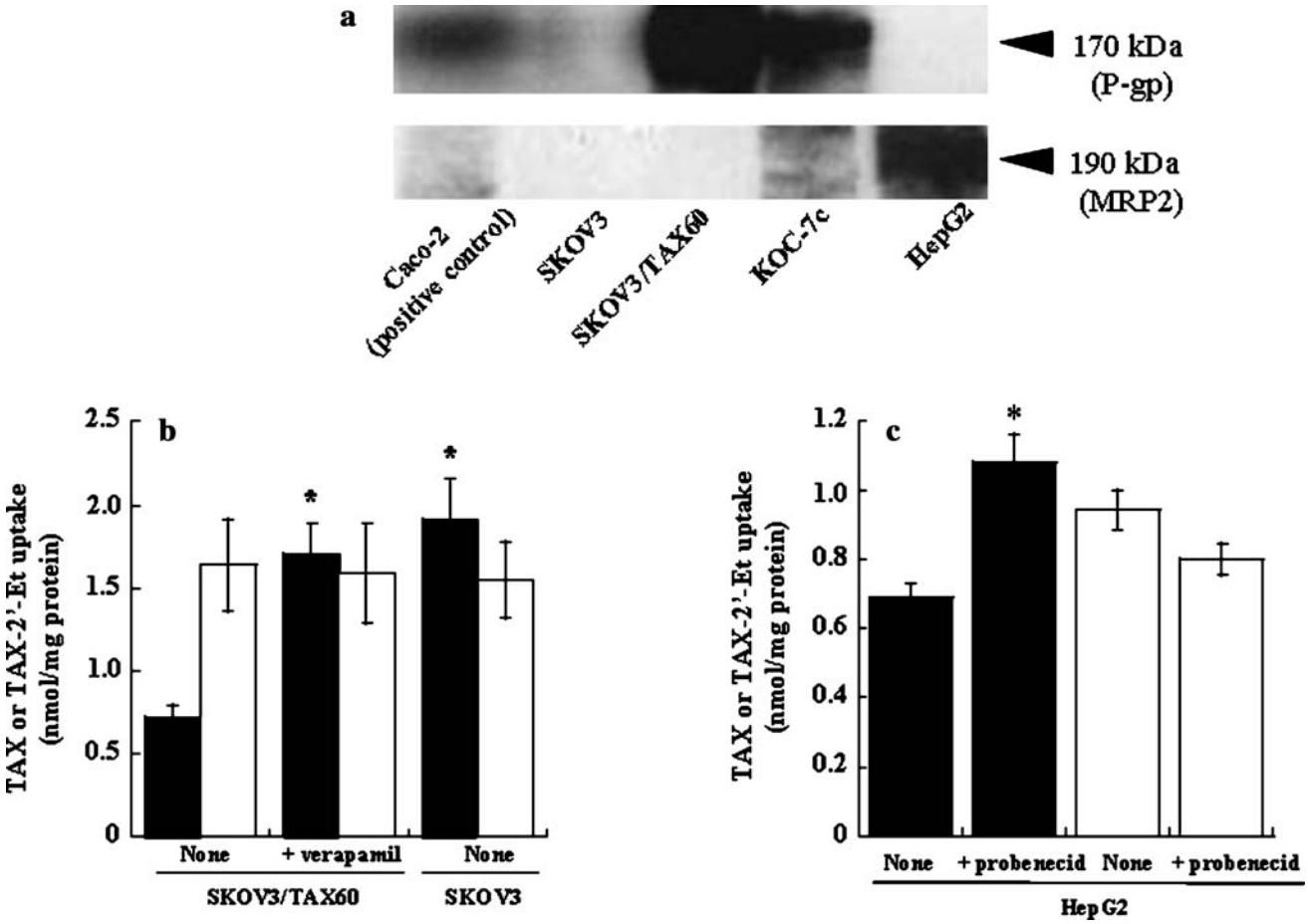

Fig. 3. Uptake of TAX and TAX-2′-Et into TAX-resistant SKOV3 and MRP2-expressing HepG2 cells. (a) Western blotting of P-gp and MRP2 expression in Caco-2, SKOV3, SKOV3/TAX60, KOC-7c and HepG2 cells. (b) SKOV3 and SKOV3/TAX60 cells were exposed for 1 h to 3.5 μM TAX (*filled columns*) or TAX-2′-Et (*open columns*) in the absence or presence of verapamil (200 μM). The results are given with standard deviation (n=3). *p<0.01, in comparison to TAX uptake after TAX exposure of SKOV3/TAX60 cells. (c) HepG2 cells were exposed for 1 h to 3.5 μM TAX (*filled columns*) or TAX-2′-Et (*open columns*) in the absence or presence of probenecid (250 μM), respectively. The results are given with standard deviation (n=3–4). *p<0.01, in comparison to TAX uptake after TAX exposure of HepG2 cells.

four hours after transfection with pHGCX or pHGCX-Ra-CES, KOC-7c cells were trypsinized and, then seeded on 96 well collagen I coated plates at a density of 5×10^4 cells. On the next day, cells were exposed to TAX or TAX-2′-Et at concentrations ranging from 7.5 to 6,000 nM. After a 72 h incubation, an MTT solution was added to each well as specified by the manufacturer.

Conversion to TAX in Ra-CES-Transfected KOC-7c Cells

After transfection of pHGCX-Ra-CES, KOC-7c cells were cultured in growth medium containing 100 nM TAX-2′-Et. We also monitored TAX accumulation in exposure of parental cells to TAX (100 nM). At the designated times (24 and 48 h), the cells were rinsed twice with ice-cold PBS. Cells were deproteinized with methanol and harvested with a cell scraper. The subsequent procedures were described in the experimental section of cell uptake. There was no change in the viability of the cells in the presence of TAX or TAX-2′-Et, and the percentage of trypan blue-stained cells was less than 5%.

Quantitation of TAX, TAX-2′-Et and Rh123

TAX and TAX-2′-Et were separated using a Cosmosil-MS 5C8 column (5 μm, 4.6×250 mm, Nacalai Tesque Co., Kyoto, Japan). HPLC analysis was performed on a system equipped with a Shimadzu SPD-10A, a UV detector, a Shimadzu LC-10A pump and a Shimadzu C-R4A chromatopac integrator. Detection was performed at 230 nm. A mobile phase of acetonitrile and 35 mM ammonium acetate buffer (pH 5.0) at a 1:1 (v/v) ratio was used at a flow rate of 1.0 ml/min.

Rh123 levels were determined by fluorescence spectrophotometry (Hitachi F4010, Tokyo, Japan). Following excitation at 507 nm, detection was performed at an emission wavelength of 529 nm.

Calculation and Statistical Analysis

Apparent permeability coefficients (P_{app}) were estimated from the slope of the linear portion of the time course of drug transport across the Caco-2 cell monolayers, as follows:

$$P_{app} = (dQ/dt)/(A\cdot C_0)$$

where dQ/dt is the permeability rate, C_0 is the initial concentration of the solute in the donor chamber and A is the surface area of the membrane.

Cytotoxicity was expressed as the concentration of drug required to induce half of the maximal cell death (EC_{50}). EC_{50} values were determined from cell survival plots using Prism software (GraphPad Software Inc., San Diego, CA, USA). Comparison of the means determined for two groups was performed using the unpaired Student's *t*-test.

RESULTS

Transport of TAX and TAX-2′-Et across Caco-2 Cell Monolayers

Caco-2 cell monolayers were confirmed based on the data that the secretory flux [from basolateral (BL) to apical (AP)] of Rh123 was five-fold greater than the absorptive flux (from AP to BL), implying that P-gp functions at the apical membrane (data not shown). Polarized transport of TAX was

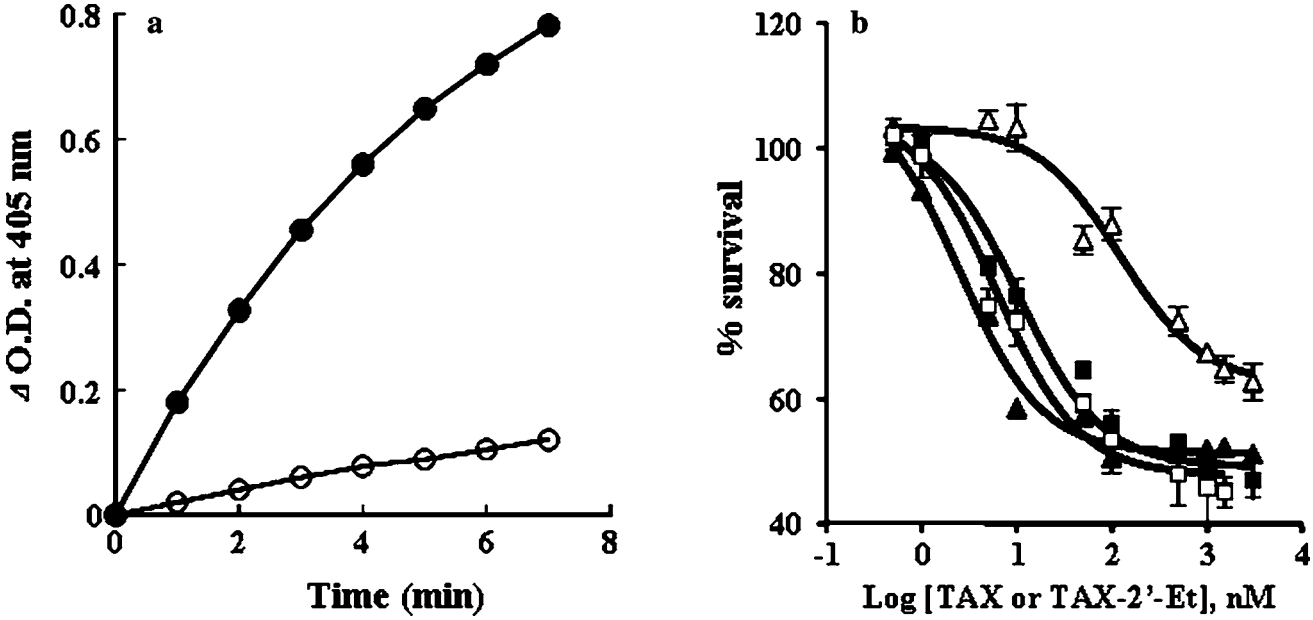

Fig. 4. Cytotoxicity of TAX and TAX-2′-Et against TAX-sensitive SKOV3 cells. (a) Time-courses of *p*-nitrophenol produced in intracellular suspensions from the transfected (*filled circle*) and untransfected cells (*open circle*) over a 48 h incubation in the Tet-off medium. The enzymatic activity plateaued at 8 min. Data points were in duplicate. (b) The number of viable untransfected (*open square*, *open triangle*) and carboxylesterase-transfected SKOV3 cells (*filled square*, *filled triangle*) was assessed by MTT assay following exposure to TAX (*squares*) or TAX-2′-Et (*triangles*). The results are given with standard deviation (n=4).

also observed under the similar conditions (Fig. 2a and b). In contrast, any differences in absorptive and secretory permeabilities of TAX-2′-Et were not observed (Fig. 2c and d). TAX-2′-Et exhibited a two-fold higher P_{app} value in the absorptive direction than TAX. The inhibitory effect of verapamil, a selective P-gp inhibitor, on the transport of both TAX and TAX-2′-Et across Caco-2 cell monolayers was also analyzed. The P_{app} values for TAX-2′-Et remained similar regardless of the presence or absence of verapamil, showing average values closed to 1.8×10^{-6} cm/s in both the absorptive and secretory directions. In contrast, the transport of TAX was strongly affected by verapamil treatment (Fig. 2a and b). For TAX, the absorptive P_{app} values increased from $0.97 \pm 0.30 \times 10^{-6}$ to 2.4±0.4 cm/s, while the secretory P_{app} decreased from $2.5 \pm 0.6 \times 10^{-6}$ to 1.8±0.4 cm/s.

Cellular Uptake of TAX and TAX-2′-Et

To elucidate contribution of P-gp to TAX-2′-Et uptake, we generated TAX-resistant SKOV3 cells (SKOV3/TAX60). Long-term exposure of TAX-sensitive SKOV3 cells to TAX induced the high expression levels of P-gp, but not MRP2 (Fig. 3a). The degree of P-gp expression in the SKOV3/TAX60 cells was comparable to that seen in another TAX-resistant KOC-7c cells. The SKOV3/TAX60 cells exhibited significantly reduced TAX uptake over a 1 h period in comparison to the TAX-sensitive SKOV3 cells (Fig. 3b). The additional of verapamil enhanced the TAX uptake into the SKOV3/TAX60 cells. In contrast, any differences in the uptake of TAX-2′-Et between the SKOV3/TAX60 cells and the SKOV3 cells were not observed.

High levels of MRP2 were expressed in HepG2 cells (Fig. 3a). The efflux of TAX-2′-Et via MRP2 transporter was studied in the presence or absence of probenecid (a inhibitor of MRP1 and 2). TAX accumulation was sensitive to probenecid (Fig. 3c). However, cellular amounts of TAX-2′-Et were not stimulated by probenecid.

Cytotoxicity and Conversion of TAX-2′-Et

The expression of functional Ra-CES in the transfected SKOV3 cells was evaluated using *p*-nitrophenyl acetate. The transfected cells exhibited nine-fold higher CES activity than the untransfected cells (Fig. 4a), indicating that the exogenous Ra-CES functions properly in the transfected cells. Higher concentrations of TAX-2′-Et were required in untransfected SKOV3 cells for growth inhibition (Fig. 4b). The cytotoxicity of TAX-2′-Et treatment (EC_{50}, 121.3 nM) was reduced 20-fold from that seen for TAX (EC_{50}, 6.2 nM) in the untransfected cells. In contrast, the induction of cell

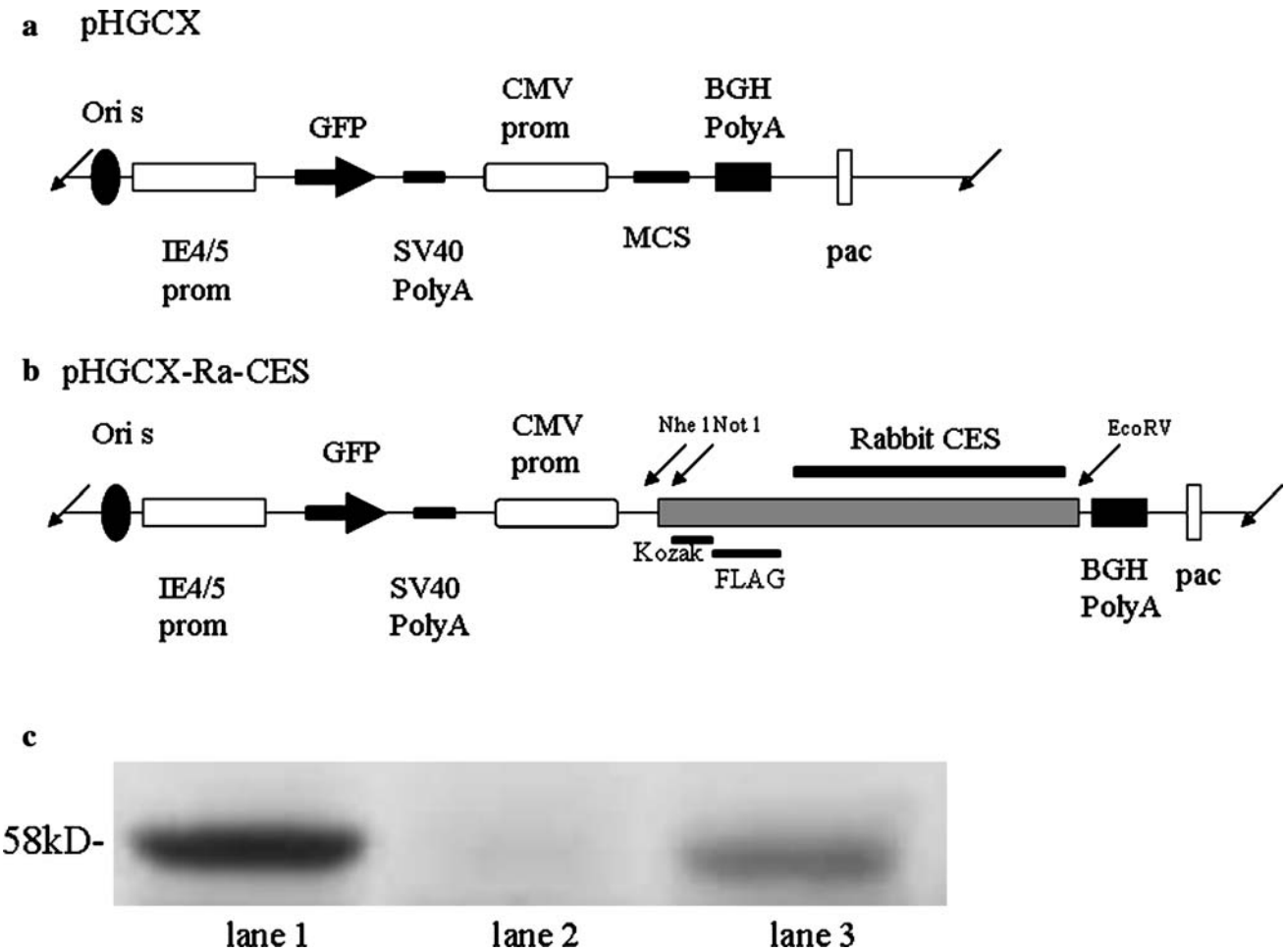

Fig. 5. Ra-CES-transfected KOC-7c cells. (a) pHGCX vector. (b) pHGCX-Ra-CES vector. (c) Immunoblot analysis of Ra-CES expression in KOC-7c cells. Fifty micrograms of the whole cell proteins of each preparation were electrophoresed. *Lane 1*, SKOV3 cells transfected with pHGCX-Ra-CES using Tet-off system; *lane 2*, pHGCX-KOC-7c cells; *lane 3*, pHGCX-Ra-CES-transfected KOC-7c cells.

death by TAX-2′-Et was markedly enhanced in the Ra-CES-transfected SKOV3 cells. In the Ra-CES-positive cells, the EC_{50} value (2.5 nM) for TAX-2′-Et was significantly lower than that (10.6 nM) obtained for TAX.

Ra-CES expression was confirmed in transient pHGCX-Ra-CES transfected KOC-7c cells by immunoblot analysis (Fig. 5c). We further estimated cytotoxicity stimulated with CES-mediated activation of TAX-2′-Et in the transfected cells (Fig. 6a). In untransfected KOC-7c cells, TAX exposures gave a EC_{50} value of more than 6.0 μM, probably responsible for high levels of P-gp but not MRP2. Transfection of the CES gene into the KOC-7c cells, however, significantly enhanced TAX-2′-Et cytotoxicity (EC_{50}, 3.0 μM). To monitor TAX-2′-Et activation relating to the enhanced cytotoxicity, we periodically measured the intracellular levels of TAX generated. Exposure to TAX-2′-Et produced significantly higher levels of intracellular TAX in comparison with exposure to TAX (Fig. 6b).

DISCUSSION

A factor limiting intracellular accumulation of both CPT-11 and its active metabolite SN38 is expression of some adenosine triphosphate (ATP)-binding cassette drug transporters [P-gp, MRP1, MRP2, MRP4 and breast cancer resistance protein (BCRP)] (22–26). To increase selectivity of CPT-11 cytotoxicity, human and rabbit CES isoenzymes are utilized in the chemotherapeutic treatment of colorectal cancer (27). However, it has been reported that the expression of BCRP protects cells from CPT-11 toxicity, even in the presence of high levels of Ra-CES that can efficiently activate the drug (28). In contrast, TAX is not substantially transported by BCRP (29). Therefore, we investigated benefit effects of TAX-2′-Et on cellular accumulation of TAX mainly mediated by P-gp, and designed an GDEPT strategy combining with TAX-2′-Et to enhance treatment potency of ovarian cancer.

Drug penetration and inhibition studies are often used to analyze the interaction between a drug and P-gp in cultured cell lines (30–33). Of the various cell lines used, Caco-2 cells have been widely accepted as a most useful *in vitro* model for rapid screening of intestinal drug absorption including P-gp dependent secretion processes (33,34). Verapamil did not alter the permeabilities of TAX-2′-Et in both the AP-to-BL and the BL-to-AP directions (Fig. 2c and d). These data indicate that, while TAX is efficiently exported from the cell by P-gp transporter, the TAX-2′-Et prodrug may escapes this pathway or reduce interaction with P-gp. Huisman *et al.* (35) have recently shown that human MRP2 transduced into a dog renal epithelia cell line (MDCKII) efficiently transported TAX. Since Caco-2 cells are known to express some exportable transporters including MRP isoforms (36), we cannot exclude contribution of MRP2 in the TAX-2′-Et transport across Caco-2 cell monolayers. Therefore, we confirmed the sensitivity of MRP2-negative and P-gp-expressing cells (SKOV3/TAX60) to TAX-2′-Et in the presence of verapamil (Fig. 3b). The uptake data strongly

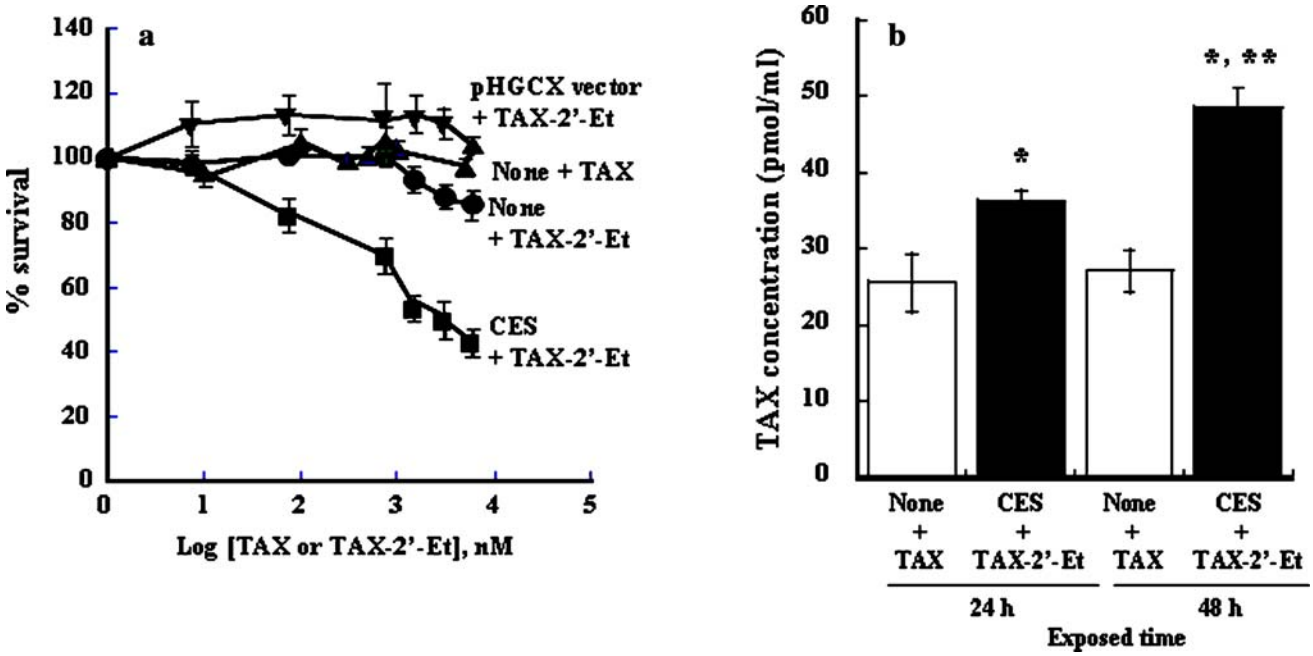

Fig. 6. Cytotoxicity of TAX and TAX-2′-Et against P-gp-expressing KOC-7c cells. (a) The number of viable parental (*filled circle*, *filled triangle*), pHGCX vector-transfected (*inverted filled triangle*), and pHGCX-Ra-CES vector-transfected KOC-7c (*filled square*) cells were assessed by MTT assay. The *closed triangles* represent exposure to TAX, while the others *three symbols* represent treatment with TAX-2′-Et. The results are given with standard deviation (n=4). (b) TAX-2′-Et activation was monitored after 24 and 48 h of exposure. *Open columns* represent TAX uptake in the parental KOC-7c cells to TAX. *Filled columns* represent the concentration of TAX activated in Ra-CES-expressing KOC-7c cells. The results are given with standard deviation (n=3). *p<0.01, in comparison to the concentration of TAX internalized after the exposure of parental KOC-7c cells to TAX. **p<0.01, in comparison to the concentration of TAX generated by a 24 h exposure of transfected cells to TAX-2′-Et.

suggest that the oxycarbonylation of the free 2′-OH group within the TAX molecule provides the ability to circumvent P-gp-associated multidrug resistance of TAX.

MRP2 transporter has a similar impact on chemotherapy as P-gp and BCRP. In the Caco-2 cells used, MRP2 expression was not detectable (Fig. 3a). However, there remains a question whether TAX-2′-Et interacts with MRP2 like TAX. Cantz *et al*. (37) have reported that HepG2 cells express high levels of MRP2 and MRP3 proteins under standard culture conditions, but MRP1 protein is not detected. We also found that MRP2 was highly expressed in HepG2 cells (Fig. 3a). Further, Cui *et al*. showed that organic anion transporters SLC21A6 (also termed OATP2, OATP-C, or LST-1) and SLC21A8 (OATP8) proteins were not detected in HepG2 cells (38). Therefore, our results suggest that TAX-2′-Et may be insensitive to MRP2 transporter.

Several TAX-2′-carbonates, but not TAX-2′-Et, are hydrolyzed at the 2′-position by nonspecific enzymes (17). It is possible that non-specific conversion of TAX-2′-Et overestimates the cytotoxicity of TAX produced by the Ra-CES enzyme. TAX-2′-Et was negligibly converted to TAX in homogenates of P-gp-negative SKOV3 cells and P-gp-positive KOC-7c cells (less than 1% of dose) (data not shown). We initially transfected Ra-CES into TAX-sensitive SKOV3 cells in order to exclude the effect of P-gp and MRP2 which can transport TAX converted from TAX-2′-Et. In the P-gp- and MRP2-negative SKOV3 cells, the stable transfection with a CES cDNA dramatically enhanced cytotoxicity of TAX-2′-Et (Fig. 4b), indicating that the exogenous Ra-CES would be a candidate available for TAX-2′-Et activation. Subsequently, we observed TAX-2′-Et activation in KOC-7c cells which express high levels of P-gp, but not MRP2. The KOC-7c cells are highly resistant to TAX, cisplatin and etoposide (19). Certainly, TAX possessed a similar EC_{50} value for the cytotoxic effect as the value (6.7 μM) reported by Itamochi *et al*. (19). In the KOC-7c cells transfected with pHGCX-Ra-CES, the cytotoxic curve after exposure to TAX-2′-Et shifted to the left in comparison to that seen in cells transfected with empty vector (Fig. 6a). In the Ra-CES-expressing KOC-7c cells, we quantitatively clarified relationship between the enhanced cytotoxicity and TAX-2′-Et conversion. TAX and TAX-2′-Et were administered at a concentration of 100 nM which induced no cell death at the designed times (24 and 48 h). It is likely that TAX produced is pumped out through P-gp transporter expressed in the Ra-CES-expressing KOC-7c cells. Actually, the accumulated intracellular TAX was available to induce a significantly higher amount of cell death. We speculate that the higher uptake of TAX-2′-Et, providing a kind of temporary reservoir for TAX, may predominates over the efflux of intracellular TAX via the P-gp transporter.

Since management of micrometastases disseminated in peritoneal cavity is extremely important in ovarian cancer, we are designing to evaluate a survival benefit and cytotoxicity of TAX-2′-Et in liver after intraperitoneal injection of TAX-2′-Et and CES-expressing vector. Intraperitoneal chemotherapy of TAX provides the ability to deliver high concentrations directly to the peritoneal space in women with advanced ovarian cancer (39), however, it cannot avoid systemic toxicity of TAX (39). If TAX-2′-Et absorbed from peritoneal cavity is not greatly activated by CES isoenzymes in liver, TAX produced may not induce severe side effects compared to intravenous injection of TAX-2′-Et. Therefore, we must clear systemic toxicity induced by TAX-2′-Et and/or TAX produced, when our GDEPT strategy is applied in *in vivo*.

Multiple forms of CESs are identified in several mammalian species. CPT-11 is converted to SN38 by a human intestinal CES, human liver CESs (called hCE1 and hCE2) and Ra-CES used presently (40). hCE2 is 64 times more efficient in CPT-11 conversion than hCE1 (41). The Ra-CES is more efficient than hCE1 (27). The Ra-CES is highly homologous to a previously cloned human CES (20) and can efficiently activate CPT-11 (28). While CES isoforms responsible for TAX-2′-Et conversion have not been identified in human and rabbit yet. Therefore, we utilized Ra-CES capable of activating TAX-2′-Et to evaluate enhanced cytotoxicity in our GDEPT strategy. The efficacy (approximately 30%) of transfection with the pHGCX-Ra-CES vector using the lipofectin system was low in the P-gp-positive KOC-7c cells (Fig. 5c). The effectiveness of this approach is apparently limited by insufficient transfection of tumor cells both *in vitro* and *in vivo*. To improve the effectiveness of the present GDEPT system, we are preparing HSV amplicon Ra-CES vectors, which may increase the transfection efficiency. Simultaneously, we will develop a GDEPT strategy utilizing human CES isoforms in order to impose minimal immunogenic risks in clinical trials.

Herpes simplex virus thymidine kinase (HSV-TK)/ganciclovir system induces cytotoxicity in neighboring HSV-TK-negative (bystander) cells (42). *In vivo*, immune system may play a role in bystander cell killing. However, induction of an immune response cannot account for bystander cytotoxicity *in vitro*. In the SKOV3/TAX60 cells, the EC_{50} value for TAX was 3.6 μM, but TAX-2′-Et did not induce any cytotoxicity even at a concentration of 5 μM. The Ra-CES-transfected SKOV3 cells were co-cultured in various ratio with the P-gp-expressing SKOV3/TAX60 cells in media containing TAX-2′-Et. When only 10% of 4×10^3 cells (total of transfected and untransfected cells) was the Ra-CES transfected SKOV3 cells, we observed 15% of growth suppression after a 72 h incubation with 5 μM of TAX-2′-Et. Subsequently, the SKOV3/TAX60 cells were incubated with the same supernatant collected as described above, showing about 10% of growth inhibition. The value was similar to the cytotoxicity data (7.5%) after a 72-h exposure of the SKOV3/TAX60 cells to 1.5 μM TAX at which the Ra-CES-transfected SKOV3 cells showed 45% of growth inhibition. In this experiment, we could not find out apparently bystander effect like HSV-TK/ganciclovir system. However, extracellular TAX produced appears to induce the cytotoxicity in the neighboring cells.

In conclusion, we provide evidence that TAX-2′-Et is able to circumvent P-gp-associated multidrug resistance. The higher cellular uptake efficiency of TAX-2′-Et, which can be converted intracellularly into TAX by Ra-CES, may be beneficial in the GDEPT for cancer cells expressing high levels of P-gp.

ACKNOWLEDGEMENTS

This study was supported in part by a research grant (No. 15591791) from the Ministry of Education, Science and

Culture of Japan. We thank Dr. T. Fujita (Kyoto Pharmaceutical University) and Dr. A. Yamamoto (Kyoto Pharmaceutical University) for their technical assistance with cell culture. We also thank Dr. Y. Saeki (Harvard Medical School) for kindly providing the pHGCX expression vector.

REFERENCES

1. E. K. Rowinsky, M. Wright, B. Monsarrat, G. J. Lesser, and R. C. Donehower. Taxol: pharmacology, metabolism and clinical implications. *Cancer Surv.* **17**:283–301 (1993).
2. W. P. Mcguire, W. J. Hoskins, M. F. Brady, P. R. Kucera, E. E. Partridge, K. Y. Look, and C. D. L. Pearson. Cyclophosphamide and cisplatin compared with paclitaxel and cisplatin in patients with stage III and stage IV ovarian cancer. *N. Engl. J. Med.* **334**:1–6 (1996).
3. J. P. Neijt, S. A. Engelholm, P. O. Witteveen, M. K. Tuxen, P. G. Sorensen, M. F. Hasen, F. Hirsch, C. Sessa, C. Swart, H. C. V. Houwelingen, B. Lund, and S. W. Hamsen. Paclitaxel (175 mg/m^2 over 3hours) with cisplatin or carboplatin in previously untreated ivarian cancer: an interim analysis. *Semin. Oncol.* **24**:36–39 (1997).
4. L. A. Martello, P. Verdier-Pinard, H. J. Shen, L. He, K. Torres, G. A. Orr, and S. B. Horwitz. Elevated level of microtuble destabilizing factors in a Taxol-resistant/dependent A549 cell line with an α-tublin mutation. *Cancer Res.* **63**:1207–1213 (2003).
5. S. Mozzetti, C. Ferlini, P. Concolino, F. Pilippetti, G. Raspaglio, S. Prislei, D. Gallo, E. Martinelli, F. O. Ranelletti, G. Ferrandina, and G. Scambia. Class III β-tublin overexpression is a prominent mechanism of paclitaxel resistance in ovarian cancer patients. *Clin. Cancer Res.* **11**:298–305 (2005).
6. A. Goncalves, K. Braguer, K. Kamath, L. Martello, C. Briand, S. Horwitz, L. Wisoni, and M. A. Jordan. Resistance to Taxol in lung cancer cells associated with increased microtuble dynamics. *Proc. Natl. Acad. Sci. U.S.A.* **98**:11737–11741 (2001).
7. B. C. Sheppard, M. J. Rutten, C. L. Meichsner, K. D. Bacon, P. O. Leonetti, J. Land, R. C. Crass, D. D. Trunkey, K. E. Deveney, and C. W. Deveney. Effect of paclitaxel on the growth of normal, polyposis, and cancerous human colonic eoithelial cells. *Cancer* **85**:1454–1464 (1999).
8. S. Roy and S. D. Horwitz. A phosphoglycoprotein associated with taxol-resistance in J7742.2 cells. *Cancer Res.* **45**:3856–3865 (1985).
9. L. A. Speicher, L. R. Barone, A. E. Chapman, G. R. Hudes, N. Laing, C. D. Smith, and K. D. Tew. P-glycoprotein binding and modulation of the multidrug resistant phenotype by estramustine. *J. Natl. Cancer Inst.* **86**:688–694 (1994).
10. K. Bhalla, Y. Huang, C. Tang, S. Self, S. Ray, M. E. Mahoney, V. Ponnathpur, E. Tourkina, A. M. Ibrado, G. Bullock, and M. C. Willingham. Characterization of a human myeloid leukemia cell line highly resistant to taxol. *Leukemia* **8**:465–475 (1994).
11. J. Van Asperen, O. Van Tellingen, M. A. ValkVan Der, M. Rozenhart, and J. H. Beijnen. Enhanced oral absorption and decreased elimination of paclitaxel in mice cotreated with cyclosporine A. *Clin. Cancer Res.* **4**:2293–2297 (1998).
12. P. B. Desai, J. Z. Duan, Y. W. Zhu, and S. Kouzi. Human liver microsomal metabolism of paclitaxel and drug interaction. *Eur. J. Drug Metab. Pharmacokinet.* **23**:417–424 (1998).
13. P. M. Fracasso, P. Westervelt, C. L. Fears, D. M. Rosen, E. G. Zuhowski, L. A. Cazenave, M. Litchman, and M. J. Egorin. Phase I study paclitaxel in combination with a multidrug resistance modulator, PSC 833 (Valspodar), in refractory malignancies. *J. Clin. Oncol.* **18**:1124–1134 (2000).
14. M. H. Kang, W. D. Figg, Y. Ando, M. V. Blagosklonny, D. Liewehr, T. Fojo, and S. E. Bates. The P-glycoprotein antagonist PSC 833 increases the plasma concentrations of 6alpha-hydroxypaclitaxel, a major metabolite of paclitaxel. *Clin. Cancer Res.* **7**:1610–1617 (2001).
15. M. Aghi, F. Hochberg, and X. O. Breakfield. Prodrug activation enzymes in cancer gene therapy. *J. Gene Med.* **2**:148–164 (2000).
16. N. F. Magri and D. G. I. Kingston. Modified Taxols. 2. Oxidation products of taxol. *J. Org. Chem.* **51**:797–802 (1986).
17. Y. Ueda, H. Wong, J. D. Matiskella, A. B. Mikkilineni, V. Farina, C. Fairchild, W. C. Rose, S. W. Mamber, B. H. Long, E. D. Kerns, A. M. Casazza, and D. N. Vyas. Synthesis and antitumor elevation of 2′-oxycarbonylpaclitaxels (paclitaxel-2′-carbonates). *Bioorg. Med. Chem.* **4**:1861–1864 (1994).
18. J. T. Spletstoser, B. J. Turunen, K. Desino, A. Rice, A. Datta, D. Dutta, J. K. Huff, R. H. Himes, K. L. Audus, A. Seelig, and G. I. Georg. Single-site chemical modification at C10 of the baccatin III core of paclitaxel and taxol C reduces P-glycoprotein interactions in bovin brain microvessel endothelial cells. *Bioorg. Med. Chem. Lett.* **16**:495–498 (2006).
19. H. Itamochi, J. Kigawa, H. Sultana, T. Iba, R. Akeshima, S. Kamazawa, Y. Kanamori, and N. Terakawa. Sensitivity to anticancer agents and resistance mechanisms in clear cell carcinoma of the ovary. *Jpn. J. Cancer Res.* **93**:723–728 (2002).
20. P. M. Potter, C. A. Pawlik, C. L. Morton, C. W. Naeve, and M. K. Danks. Isolation and partial characterization of a cDNA encoding a rabbit liver carboxylesterase that activatives the prodrug irinotecan (CPT-11). *Cancer Res.* **58**:2646–2651 (1998).
21. I. Hennebelle, C. Terret, E. Chatelut, R. Bugat, P. Canal, and S. Fguichard. Characterization of CPT-11 converting carboxylesterase activity in colon tumor and normal tissues: comparison with p-nitro-phenylacetate converting carboxylesterase activity. *Anti-cancer Drugs* **11**:465–470 (2000).
22. A. K. Lalloo, F. R. Luo, A. Guo, P. V. Paranjpe, S. H. Lee, V. Vyas, E. Rubin, and P. J. Sinko. Membrane transport of camtothecin: facilitation by human P-glycoprotein (ABCB1) and multidrug resistance protein 2 (ABCC2). *BMC Med.* **4**:2–16 (2004).
23. F. R. Luo, P. V. Paranjpe, A. Guo, E. Rubin, and P. Sinko. Intestinal transport of irinotecan in Caco-2 cells and MDCK II cells overexpressing efflux transporters Pgp, cMOAT, and MRP1. *Drug Metab. Dispos.* **30**:763–770 (2002).
24. X. Y. Chu, Y. Kato, and Y. Sugiyama. Multiplicity of biliary excretion mechanisms for irinotecan, CPT-11, and its metabolites in rats. *Cancer Res.* **57**:1934–1938 (1997).
25. M. D. Norris, J. Smith, K. Tanabe, P. Tobin, C. Flemming, G. L. Scheffer, P. Wielinga, S. L. Cohn, W. B. London, G. M. Marshall, J. D. Allen, and M. Haber. Expression of multidrug transporter MRP4/ABCC4 is marker of poor prognosis in neuroblastoma and confers resistance to irinotecan *in vitro*. *Mol. Cancer Ther.* **4**:547–553 (2005).
26. C. J. Yang, J. K. Horton, K. H. Cowan, and E. Schneider. Cross-resistance to camptothecin analogues in a mitoxantrone-resistant human breast carcinoma cell line is not due to DNA topoisomerase I alterations. *Cancer Res.* **55**:4004–4009 (1995).
27. M. K. Danks, C. L. Morton, E. J. Krull, P. J. Cheshire, L. B. RichmondI, C. W. Naeve, C. A. Pawlik, P. J. Houghton, and P. M. Potter. Comparison of activation of CPT–11 by rabbit and human carboxylesterases for use in enzyme/prodrug therapy. *Clin. Cancer Res.* **5**:917–924 (1999).
28. M. Wierdl, A. Wall, C. L. Morton, J. Sampath, M. K. Danks, J. D. Schuetz, and P. M. Potter. Carboxylesterase-mediated sensitization of human tumor cells to CPT-11 cannot override ABCG2-mediated drug resistance. *Mol. Pharmacol.* **64**:279–288 (2003).
29. L. A. Doyle and D. D. Ross. Multidrug resistance mediated by the breast cancer resistance protein BCRP (ABCG2). *Oncogene* **22**:7340–7358 (2003).
30. A. H. Dantzing, R. L. Shepard, J. Cao, K. L. Law, W. J. Ehlhardt, T. M. Baighman, T. F. Bumol, and J. J. Starling. Reversal of P-glycoprotein-mediated multidrug resistance by a potent cyclopropyldibenzosuberane modulator, LY335979. *Cancer Res.* **56**:4171–4179 (1996).
31. M. Shionoya, T. Jimbo, M. Kitagawa, T. Soga, and A. Tohgo. DJ-927, a novel oral taxane, overcomes P-glycoprotein-mediated multidrug resistance *in vitro* and *in vivo*. *Cancer Sci.* **94**:459–466 (2003).
32. S. H. Jang, M. G. Wientjes, and J. L.-S. Au. Kinetics of P-glycoprotein-mediated efflux of paclitaxel. *J. Pharmacol. Exp. Ther.* **298**:1236–1242 (2001).
33. D. Schwab, H. Fischer, A. Tabatabaei, S. Poli, and J. Huwyler. Comparison of *in vitro* P-glycoprotein screening assays: recom-

mendations for their use in drug discovery. *J. Med. Chem.* **46**:1716–1725 (2003).
34. R. Yumoto, T. Murakami, Y. Nakamoto, R. Hasegawa, J. Nagai, and M. Takano. Transport of rhodamine 123, a P-glycoprotein substrate, across rat intestine cell and Caco-2 cell monolayers in the presence of cytochrome P-450 3A-related compounds. *J. Pharmacol. Exp. Ther.* **289**:149–155 (1999).
35. M. T. Huisman, A. A. Chhatta, O. V. Tellingen, J. H. Beijnen, and A. H. Schinkel. MRP2 (ABCC2) transports and confers paclitaxel resistance and both processes are stimulated by probenecid. *Int. J. Cancer* **116**:824–829 (2005).
36. H. M. Prime-Chapman, R. A. Fearn, A. E. Cooper, V. Moore, and B. H. Hirst. Diferential multidrug resistance-associated protein 1 through 6 isoform expression and function in human intestinal epithelial Caco-2 cells. *J. Pharmacol. Exp. Ther.* **311**:476–484 (2004).
37. T. Cantz, A. T. Nies, M. Brom, A. F. Hofmann, and D. Keppler. MRP2, a human conjugate export, is present and transports flu 3 into apical vacuoles of Hep G2 cells. *Am. J. Physiol.: Gastrointest. Liver Physiol.* **278**:G522–G533 (2000).
38. Y. Cui, J. Konig, A. T. Nies, M. Pfannschmidt, M. Hergt, W. W. Franke, W. Alt, R. Moll, and D. Keppler. Detection of the human organic anion transporters SLC21 (OATP2) and SLC21A8 (OATP8) in liver and hepatocellular carcinoma. *Lab. Invest.* **83**:527–538 (2003).
39. M. Markman, E. Rowinsky, T. Hakes, B. Reichman, W. Jones, J. L. Jr. Lewis, S. Rubin, J. Curtin, R. Barakat, M. Phillips, *et al.* Phase I trial of intraperitoneal taxol: a gynecologic oncology group study. *J. Clin. Oncol.* **10**:1485–1491 (1992).
40. K. J. Yoon, J. L. Hyatt, C. L. Morton, R. F. Lee, P. M. Potter, and M. K. Danks. Characterization of inhibitors of specific carboxylesterases: development of carboxylesterase inhibitors for translational application. *Mol. Cancer Ther.* **3**:903–909 (2004).
41. R. Humerckhouse, K. Lohrbach, L. Li, W. F. Bosron, and M. E. Dolan. Characterization of CPT-11 hydrolysis by human liver carboxylesterase isoforms hCE-1 and hCE-2. *Cancer Res.* **60**:1189–1192 (2000).
42. L. Z. Rubsam, P. D. Boucher, P. J. Murphy, M. KuKuruga, and D. S. Shewach. Cytotoxicity and accumulation of ganciclovir triphosphate in bystander cells cocultured with herpes simplex virus type 1 thymidine kinase-expressing human glioblastoma cells. *Cancer Res.* **59**:669–675 (1999).